Proceedings of IMECE2006
2006 ASME International Mechanical Engineering Congress and Exposition
November 5-10, 2006, Chicago, Illinois, USA

IMECE2006-16103

THE *RiceWrist*: A DISTAL UPPER EXTREMITY REHABILITATION ROBOT FOR STROKE THERAPY

Marcia K. O'Malley*
Alan Sledd
Abhishek Gupta
Volkan Patoglu
Joel Huegel
Department of Mechanical Engineering
Rice University, Houston, Texas 77005
{omalleym, amsledd, abhi, vpatoglu, jhuegel}@rice.edu

Charles Burgar, MD
CTVHCS
Temple, Texas 76504
charles.burgar1@med.va.gov

ABSTRACT

This paper presents the design and kinematics of a four degree-of-freedom upper extremity rehabilitation robot for stroke therapy, to be used in conjunction with the Mirror Image Movement Enabler (MIME) system. The RiceWrist *is intended to provide robotic therapy via force-feedback during range-of-motion tasks. The exoskeleton device accommodates forearm supination and pronation, wrist flexion and extension, and radial and ulnar deviation in a compact design with low friction and backlash. Joint range of motion and torque output of the electric-motor driven device is matched to human capabilities. The paper describes the design of the device, along with three control modes that allow for various methods of interaction between the patient and the robotic device. Passive, triggered, and active-constrained modes, such as those developed for MIME, allow for therapist control of therapy protocols based on patient capability and progress. Also presented is the graphical user interface for therapist control of the interactions modes of the* RiceWrist*, basic experimental protocol, and preliminary experimental results.*

INTRODUCTION

Each year 500,000 people in the United States survive cerebral vascular accident (CVA), or stroke, with the total number of survivors now approaching two million. The estimated cost for rehabilitation and lost revenue exceeds $7 billion per year. Stroke commonly causes significant residual physical, cognitive, and psychological impairment [1]. As the geriatric population increases and more effective therapies for acute stroke management emerge, there will be more survivors living with disabilities. There has also been a trend toward more moderately affected survivors [2], which has increased the demand for stroke rehabilitation in an era of health care cost containment. Persons with hemiparesis following stroke constitute the largest group of patients receiving rehabilitation services in this country. Efforts to prevent stroke must, therefore, be balanced with pragmatic efforts to prevent disability and maximize quality of life for stroke survivors. Current consensus regarding rehabilitation of patients with some voluntary control over movements of the paretic limb is that they be encouraged to use the limb in functional tasks and receive training directed toward improving strength and motor control, relearning sensorimotor relationships, and improving functional performance [3]. Research efforts that improve the effectiveness of rehabilitative treatment of motor disability resulting from stroke are needed. With the dramatic reduction of inpatient rehabilitation length of stay following stroke, efficient and effective interventions have become critical.

*All correspondence should be addressed to this author

Robotic Rehabilitation Systems

Interest in the rehabilitation applications for robots has been increasing [4–6]. Khalili and Zomlefer suggested that a two joint robot system could be used for continuous passive motion and could be programmed to the particular needs of the patient [7]. Goodall et al. used two single degree-of-freedom (DOF) arms to stabilize sway in hemiparetic patients, and suggested the level of assistance could be withdrawn to encourage patients to relearn to balance on their own [8]. White et al. built a single DOF pneumatically powered orthotic device for elbow flexion that could be used for continuous passive motion, to measure patient strength, and to assist elbow flexion [9]. Dirette et al. showed that a continuous passive motion (CPM) machine, when used regularly, can effectively reduce edema in the hands of flaccid hemiparetic patients [10]. As described here, the majority of robotic rehabilitation systems to date have focused on upper-extremity, specifically the shoulder and/or elbow.

Prior work has studied the ability of a device (Mirror-Image Motion Enabler – MIME) [11] to assist limb movements and facilitate recovery of motor function in subjects with chronic hemiparesis due to stroke. MIME incorporates an industrial robot and operates in three unilateral modes and one bimanual mode. In unilateral operation, passive, active-assisted, and guided movements against a resistance are possible. The bimanual mode enables the subject to practice bilateral, coordinated movements with rate and range under his or her control.

In the current version of MIME, subjects are seated in a wheelchair modified to improve seating support and reduce movements of the upper body. They can sit close to either the front or rear of an adjustable height table. A PUMA-560 robot is mounted beside the table. It is attached to a wrist-forearm orthosis (splint) via a 6-axis force transducer, a pneumatic breakaway overload sensor set to 20 Nm torque, and a quick-release coupling mechanism. The subject's arm is strapped into the splint with the wrist in neutral position. Robot/forearm interaction force and torque measurements from the transducer are recorded and archived by a personal computer. The control program monitors these data and the motion of the robot in order to prevent potentially hazardous situations from occurring. Switches and mechanical stops are strategically placed to permit rapid deactivation of the robot, if necessary.

In an initial study with MIME including twenty-eight subjects (two groups of 14) all had improved motor function as a result of therapy [11]. The robot group, compared to the control group, had larger improvements in the proximal movement portion of the Fugl-Meyer (FM) test after one month of treatment and also after two months of treatment. The robot group also had larger gains in strength and larger increases in reach extent after two months of treatment. At the six-month follow-up, the groups no longer differed in terms of the Fugl-Meyer test, however the robot group had larger improvements in the FIM (Functional Independence Measure).

Preliminary data from these ongoing clinical efficacy trials suggest that robot-aided therapy has therapeutic benefits. Improvements have been demonstrated in strength and in the FM assessment of motor function. Trends in the data suggest that the underlying mechanisms for these results may be increased strength, as well as more appropriate activation and inhibition of muscle groups.

The reader is referred to extensive reviews of robotic therapy for upper and lower extremity for a more complete discussion of the state of the field [12–17].

The MIME studies together with the cited related work support the conclusions that robotic manipulation of an impaired limb may favorably affect recovery following a stroke. An important additional finding is that improvements in motor control are possible beyond six months following a stroke.

Such findings with shoulder and elbow rehabilitation motivate the extension of robotic-assisted rehabilitation distally for the upper extremity, so that forearm pronation-supination, wrist flexion-extension, radial-ulnar deviation, and ultimately digital manipulation are enabled. Several devices have been presented in the literature to achieve at least a subset of these movements. For example, Charles et al. [18] have developed an extension of the MIT-MANUS system to provide three rotational degrees-of-freedom for wrist rehabilitation. Hesse et al. [19] have also extended the utility of their arm trainer to include wrist motion. In order to improve the applicability of the MIME system for full arm rehabilitation post stroke, the authors have developed the *RiceWrist*, a modification of the MAHIexoskeleton [20, 21], which interfaces with MIME and provides a variety of interaction modes for the therapist to select for the patient.

The recently developed *RiceWrist* has been integrated with the MIME system to extend the three unilateral operation modes to include forearm supination and pronation, wrist flexion and extension, and radial and ulnar deviation. The device design extends from prior work by some of the authors. A thorough discussion of specific design considerations for the original MAHI exoskeleton and how each was addressed can be found in [20]. The redesign of the MAHI exoskeleton, discussed in [21], successfully addresses the limitations of the original device design. Further refinement of the *RiceWrist* design including the mechanical interfacing with MIME will be discussed in this paper. Performance results for the interaction modes of the *RiceWrist* are also presented.

DESIGN OF THE *RiceWrist*

The *RiceWrist* is an electrically actuated forearm and wrist haptic exoskeleton device that has been designed for rehabilitation applications. The kinematic design of the *RiceWrist* allows for reproduction of most of the natural human wrist and forearm workspace, force isotropy and high torque output levels required during robot-aided rehabilitation. Another important feature of

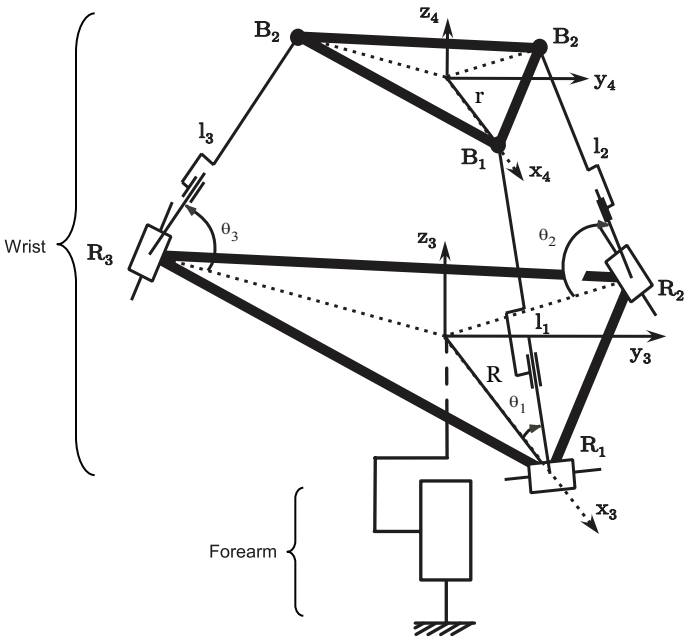

Figure 1. *RiceWrist* mechanism: A 3-RPS platform is used as the wrist of the robot. Joints R_1, R_2 and R_3; and B_1, B_2 and B_3 are located at vertices of equilateral triangles.

the design is the alignment of the axes of the rotation of human joints with the controlled degrees-of-freedom of the exoskeleton. The problem of measurement of arm position is thus reduced to the solution of the exoskeleton kinematics, with no further transformations required. This makes it possible to actuate the robot to control feedback to a specific human joint, for example to constrain the forearm rotation during wrist rehabilitation, without affecting other joints.

Robot-aided rehabilitation typically requires the use of virtual force fields for guidance or active assistance. The *RiceWrist* has high force output bandwidth, low backlash, low-friction, high backdrivability, high structural stiffness and a singularity free workspace, features characteristic of a high quality haptic interface. The absence of singularities in the workspace ensures that the forward and inverse kinematics of the robot can be solved uniquely at each point, thus making the measurement of arm position and force feedback easier.

The basic kinematic structure of the *RiceWrist* is depicted in Fig. 1. The exoskeleton is comprised of a revolute joint at the forearm and a 3-RPS (revolute-prismatic-spherical) serial-in-parallel wrist. The 3-RPS platform, mentioned in Lee and Shah [22], consists of a base plate, three extensible links l_1, l_2 and l_3 and a moving plate. The moving plate houses the end-effector that is affixed to the operator during operation. The moving plate is connected to the three extensible links by means of spherical joints spaced at 120° along the circumference of a circle of radius r. The other end of the links connects to the base plate via revolute (pin) joints, which are also spaced at 120° along a circle of radius R. The axes of rotation of the revolute joints are oriented along the tangents to this circle. Actuators placed along the link are used to change the link length, thereby moving the top plate. It should be noted that the platform has limited translational movement transverse to the vertical axis through the base and no singularities for $\theta_i \in (0, \pi)$ [22]. The device has four degrees of freedom corresponding to the rotation of the forearm, height of the wrist platform and 2 DOF in rotation of the top plate of the platform with respect to to the base plate.

The choice of a parallel mechanism for the design of the *RiceWrist* over a serial mechanism was motivated primarily by the compactness of the parallel mechanism. Furthermore, use of a parallel mechanism allows for higher torque output, stiffness, and decreased inertia as compared to a similar serial mechanism. The parameters of the platform were optimized to limit the size of the mechanism [20].

During operation, the robot is worn such that the top plate of the wrist of the robot aligns with the wrist joint of the operator. This configuration aids in preserving natural arm movements by aligning the robot's kinematic structure with that of the human arm. Velcro strapping and adjustable ergonomic upper forearm and palm splints are used to maintain the axes alignment. The mapping between the robot configuration and arm position is further simplified by the use of the 3-RPS kinematic structure for the robot.

Wrist Kinematics

For the purpose of analysis, the coordinate axes are fixed to various joints of the exoskeleton, as shown in Fig. 1. Frames $\{3\}$ and $\{4\}$ are fixed to the bottom and top plates of the platform, respectively.

Now, given the transformation matrix between frames $\{3\}$ and $\{4\}$, the position and orientation of the wrist platform can be computed, which provides the position and orientation of the human wrist. The equivalence between the human wrist joint angles and the *xyz* Euler angle representation for the orientation of the platform is shown in the following subsection.

As shown in Fig. 1, the base coordinate frame, $\{3\}$, is attached to the center of the base platform with the z_3-axis pointing vertically upwards and x_3-axis towards the first revolute joint, R_1. Frame, $\{4\}$ is attached to the moving platform with the z_4-axis being normal to the platform and the x_4-axis pointing towards the first spherical joint, B_1. Using Grashof's criterion it can be shown that the system has three degrees of freedom. Furthermore, due to the constraint imposed by the revolute joints, the rotation of the platform about axis z_4 is not possible. Hence, the platform has only two degrees of freedom in orientation and one in translation. The length of individual links are denoted by l_i. The homogeneous transformation matrix ${}^4T_3$, which represents

$\{4\}$ in terms of the base frame, $\{3\}$ is

$$^3T_4 = \begin{bmatrix} n_1 & o_1 & a_1 & x_c \\ n_2 & o_2 & a_2 & y_c \\ n_3 & o_3 & a_3 & z_c \\ 0 & 0 & 0 & 1 \end{bmatrix} \quad (1)$$

where $(x_c, y_c, z_c)^T$ denotes the position of the origin of frame $\{4\}$ in the base frame. The direction cosines of the unit vectors *x*, *y*, and *z* in the base frame are represented by $(n_1, n_2, n_3)^T$, $(o_1, o_2, o_3)^T$, and $(a_1, a_2, a_3)^T$. For subsequent analysis, all coordinates and lengths have been normalized using the base radius, *R*. The following are defined:

$$\rho = \frac{r}{R} \quad L_i = \frac{l_i}{R} \quad (2)$$

then

$$X_c = \frac{x_c}{R} \quad Y_c = \frac{y_c}{R} \quad Z_c = \frac{z_c}{R} \quad (3)$$

Forward Kinematics The forward kinematics for the platform involves solving simultaneous equations for the position and orientation of the movable platform in terms of the given link lengths. The fact that the manipulator is essentially a structure for fixed lengths has been used to derive these equations. If θ_i is the angle between link R_iB_i, then, the distance between any two spherical joints, $\sqrt{3}r$, can be used to implicitly relate θ_i to L_i. This leads to three constraint equations given as

$$L_1^2 + L_2^2 - 3 - 3\rho^2 + L_1L_2\cos\theta_1\cos\theta_2 - 2L_1L_2\sin\theta_1\sin\theta_2 - 3L_1\cos\theta_1 - 3L_2\cos\theta_2 = 0 \quad (4)$$

$$L_3^2 + L_2^2 - 3 - 3\rho^2 + L_3L_2\cos\theta_3\cos\theta_2 - 2L_3L_2\sin\theta_3\sin\theta_2 - 3L_3\cos\theta_3 - 3L_2\cos\theta_2 = 0 \quad (5)$$

$$L_1^2 + L_3^2 - 3 - 3\rho^2 + L_1L_3\cos\theta_1\cos\theta_3 - 2L_1L_3\sin\theta_1\sin\theta_3 - 3L_1\cos\theta_1 - 3L_3\cos\theta_3 = 0 \quad (6)$$

Multiple solutions of θ_1, θ_2 and θ_3 for a given set of link lengths are possible. A further mathematical constraint

$$0^\circ < \theta_i < 180^\circ$$

ensures uniqueness. In other words, position z_c for the platform must always be positive, i.e., the moving platform should always move on one side of the base platform, a physical constraint. With this constraint, Eqns. 4-6 can be solved numerically for θ_i.

As the spherical joints are placed at the vertices of an equilateral triangle, the Cartesian position of the origin of the moving frame $\{4\}$, which is the centroid of the triangle, C can be calculated.

The Cartesian position of the spherical joints can be expressed as

$$\begin{bmatrix} ^4B_i \\ 1 \end{bmatrix} = ^4T_3 \begin{bmatrix} ^3B_i \\ 1 \end{bmatrix} \quad (7)$$

Furthermore, the coordinates of the spherical joints with respect to the base frame are

$$^3B_1 = \begin{bmatrix} 1 - L_1\cos\theta_1 \\ 0 \\ L_1\sin(\theta_1) \end{bmatrix} \quad ^3B_2 = \begin{bmatrix} \frac{-1}{2}(1 - L_2\cos\theta_2) \\ \frac{\sqrt{3}}{2}(1 - L_2\cos\theta_2) \\ L_2\sin(\theta_2) \end{bmatrix}$$

$$^3B_3 = \begin{bmatrix} \frac{-1}{2}(1 - L_3\cos\theta_3) \\ \frac{-\sqrt{3}}{2}(1 - L_3\cos\theta_3) \\ L_3\sin(\theta_3) \end{bmatrix} \quad (8)$$

Eqns. 7 and 8 can be solved to determine the vectors **n**, **o** and **a** and hence the orientation of the platform. Once the transformation matrix *T* is known, the orientation of the platform in terms of *xyz*-Euler angles, α, β, and γ, can be determined using

$$\beta = \sin^{-1}(n_3) \quad \alpha = Atan2(-o_3/\cos(\beta), a_3/\cos(\beta))$$

$$\gamma = Atan2(-n_2/\cos(\beta), n_1/\cos(\beta))$$

It should be noted that if $\beta = \pm 90^\circ$, α and γ become indeterminate. In addition, the top plate of the platform cannot rotate about z_4 and hence, $\gamma = 0$ in general. For a detailed discussion of forward kinematics, please refer to [20].

Inverse Kinematics As the moving platform has three degrees of freedom, its position can be defined in terms of the first two *xyz*-Euler angles, α, β and one Cartesian coordinate, Z_c. As the links R_1B_1, R_2B_2 and R_3B_3 are constrained by the revolute joints to move in the planes $y = 0, y = -\sqrt{3}x$, and $y = \sqrt{3}x$ respectively, using Eqn. 7 we have

$$n_2\rho + Y_c = 0; \quad X_c = \frac{\rho}{n_1 - o_2}$$

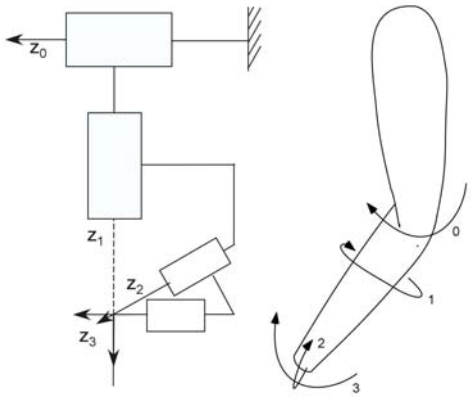

Figure 2. Simplified kinematic model of the human arm: Other axes have not been shown for clarity. Axes 0 through 3 represent elbow rotation, forearm rotation, wrist adduction/abduction and wrist flexion/extension respectively.

Now, $\gamma = 0$, as the top plate of the platform cannot rotate about z_4. Hence, X_c, Y_c and γ can be easily solved. The orientation and position of the top plate can then be used to compute the transformation matrix, T and determine the Cartesian positions, B_i using Eqn. 7. The actuator position is then trivial to calculate as the length of link R_iB_i.

Measurement of Human Wrist Joint Angles

A simplified kinematic model of the human lower arm and the wrist is shown in Fig. 2. Notice that axes x_4 of the platform (see Fig. 1) and z_2 of the human wrist joint coincide when the exoskeleton is worn by an operator. Similarly, axes y_4 of the platform and z_3 of the arm coincide for any rotation, α, of the top plate of the platform about x_4, or of the human wrist about z_2 (Fig. 2). Furthermore, $\{3\}$ of the platform has a fixed orientation with respect to $\{1\}$ of the human arm. Hence, a rotation of the top plate of the platform about axis x_4 (Fig. 1) followed by another rotation about axis y_4 (Fig. 1), is equivalent to a transformation from $\{3\}$ to $\{1\}$ of the arm. This implies that with the top plate of the platform centered at the operator's wrist joint, the measurement of the orientation of the top plate with respect to the base of the platform in terms of *xyz*-Euler angles corresponds to measurement of the flexion/extension and abduction/adduction of the human wrist joint. Thus, the Euler angle of rotation α about axis x_4 corresponds to abduction/adduction of the wrist while the rotation angle β about y_4 corresponds to flexion/extension. The forearm joints of the robot and human being coincident, the measurement of position of operator's elbow and forearm from robot coordinates and vice versa is trivial as shown in the previous section.

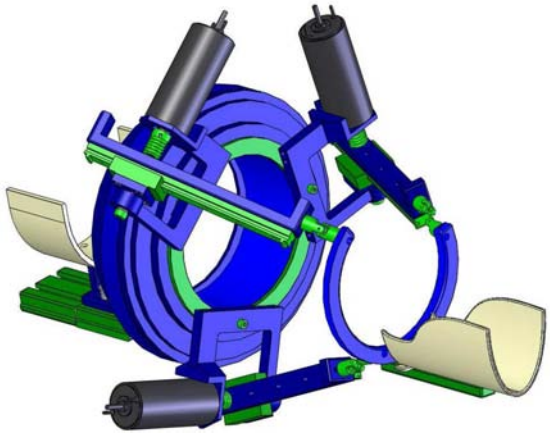

Figure 3. Rendering of the mechanical design of the *RiceWrist*

Mechanical Design of the *RiceWrist*

Figure 3 depicts the 3-D rendering of the final design. The actuator for the forearm is a brushless permanent magnet frameless motor supplied by Applimotion providing 1.7 Nm continuous and 5.1 Nm peak torque with a 16,000 count/turn digital encoder (MicroE Systems). The wrist platform link lengths are varied via high torque rotary electric motors and cable-driven (capstan) mechanisms. Three lightweight Maxon RE30 motors were chosen for high torque output along with precision 500 count/turn digital encoders. With the capstan transmission that, by design, is backdriveable and free of backlash, the Maxon motor and transmission assembly within the 3-RPS platform is able to meet torque, friction and range of motion requirements presented in Table 1. Because stroke patients typically have some degree of tone, the parallel wrist platform required a horseshoe design to allow ease of donning while not affecting the stiffness of the device. Furthermore, the *RiceWrist* is mounted on the end effector of MIME via a quick release mechanism that facilitates switching from the right to the left hand and vice-versa.

The *RiceWrist* has been developed with the safety of the subject at the forefront of each design decision. Emergency stops are provided for both subject (foot pedal) and therapist (push button) which disarm a relay on the power side of the amplifiers. Adjustable position soft stops and mechanical hard stops are provided for each actuator as well as torque limits in software. For redundancy, torque limits are also set in the amplifiers.

REHABILITATION SETUP

Figure 4 shows the overall setup for the MIME-*RiceWrist* rehabilitation system. The therapist maintains high level supervisory control over the therapy session. The therapist can customize the physical therapy sessions according to the needs of individual patients.

A graphical user interface (GUI), as shown in Fig. 5, is pro-

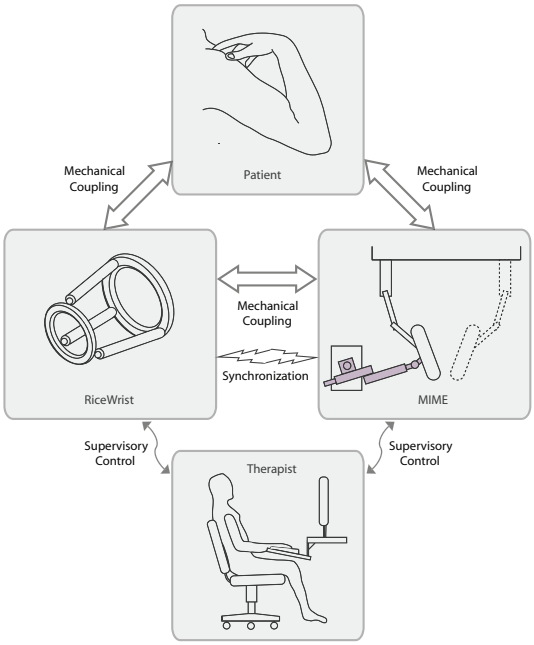

Figure 4. MIME- *RiceWrist* rehabilitation system setup

vided to the therapist to facilitate customization of the sessions. The GUI provides an interface to record patient information and individual session details. Prior to a therapy session, the therapist can record the joint limits of the patient to plan the desired start and end positions for reaching movements. This information is also stored on a local file for future reference and updates. For each trial, the therapist can then choose the desired trajectory by selecting start and end positions, number of repetitions and the speed of travel. Three different modes of operation – passive, triggered and constrained – are implemented on the system. Through the GUI, the therapist can also select the mode of operation and associated parameters.

Control Modes

Three control modes that match the control modes of the MIME system – passive, triggered or constrained, have been implemented on the *RiceWrist*. Figure 6 depicts the structure of the controller for the MIME-*RiceWrist* system. The system has five modes of operation, three of which are the aforementioned control modes. The other modes are GoTo and Wait. When operating in the GoTo mode, the system moves to an initial position, which is specified by the therapist. On reaching the desired position, the system switches to the Wait mode, in which a virtual fixture is used to restrict arm movement, until the therapist initiates or resumes the trial. Following the command from the therapist, the system switches to one of the three control modes until the desired end position for the trial is reached. Upon reaching this position, the system switches back to the Wait mode until

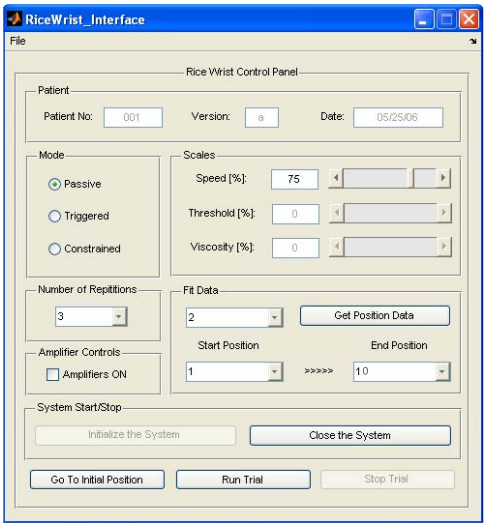

Figure 5. Graphical user interface for the therapist

the therapist commands to initiate the return motion. This process can be repeated for the desired number of repetitions. Please note that the therapist selects the initial and final positions in an initial sizing session for each patient.

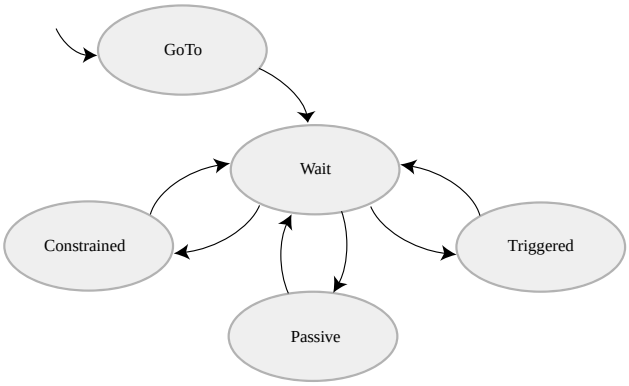

Figure 6. Structure of the switching controller for the MIME- *RiceWrist* System

The **GoTo mode** is implemented as a joint-space trajectory controller, as shown in Fig. 7. The desired trajectory is computed through linear interpolation using the current and specified initial positions. Note that the initial and final positions are prerecorded by the therapist.

The **Wait mode** is implemented as a task-space impedance force controller, as shown in Fig. 8. Note that it is assumed that the velocities of motion are small enough to ignore the dynamic terms in the equations of motion of the device. A high stiffness virtual wall prevents arm motions until a new mode is activated.

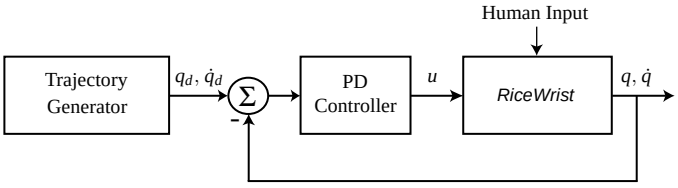

Figure 7. PD trajectory controller for the *RiceWrist* System, where, q_d, $\dot{q}_d$ are the desired joint position and velocities; q, $\dot{q}$ are the current joint position and velocities; and u is the control input.

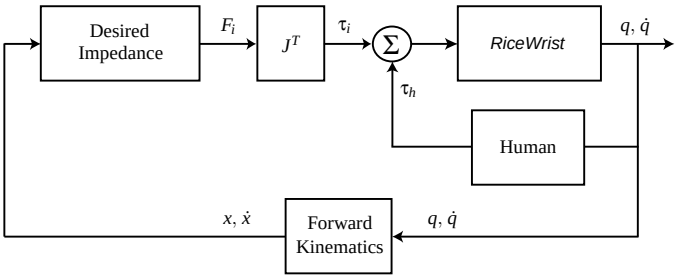

Figure 8. Task-space impedance controller for the *RiceWrist* System, where, q, $\dot{q}$ are the current joint position and velocities; x, $\dot{x}$ are the current task-space position and velocities; F_i is the desired environment force; J is the Jacobian of the *RiceWrist* ; τ_i is the desired joint torques; and τ_h is the human induced joint torque.

The **Passive mode** is similar to the GoTo mode where the device guides the patient to a desired end position. The desired trajectory is computed through linear interpolation using the start and end positions. The trajectory is also time scaled with the selected speed of travel.

The **Triggered mode** is a modified form of the Passive mode in which the patient must overcome a pre-specified force threshold in the Wait mode to initiate motion. Once the force threshold is overcome the device behaves as in the passive mode.

The **Constrained mode** is implemented as a task-space impedance force controller as used for the Wait mode. Unlike the Passive and Triggered modes, which are passive, this is an active mode where the patient is required to actively move his arm to the end position. Once movement has been initiated along the trajectory motion reversal is restricted by implementation of a virtual wall in that direction. Resistive impedance can also be displayed to the patient along the trajectory to provide strength training.

Controller Implementation

The *RiceWrist* controller runs on a 3.2 GHz Pentium 4 PC with 2GB of RAM. To free up processor time, a 128MB graphics card (AGP) was selected. The hardware is controlled through the MATLAB Real Time Workshop Toolbox from Mathworks, and WinCon from Quanser Consulting. All data acquisition is handled by Quanser's Q8 board, designed specifically for hardware in the loop applications. The Quanser board features 14-bit input, simultaneous sampling of A/D and encoder inputs, and extensive input/output options (8 each of A/D, D/A, encoder and 32 DIO). MIME and *RiceWrist* communicate through the serial port. Communication is mainly for synchronization of start and end of trials.

RESULTS AND DISCUSSION

Figure 9 shows a subject operating the MIME-*RiceWrist* integrated system. Velcro strapping and a molded splint are used to attach the subject's arm to the device. The following subsection provides mechanical performance characteristics of the *RiceWrist*. Performance of the *RiceWrist* under position and force control is discussed in the concluding subsection.

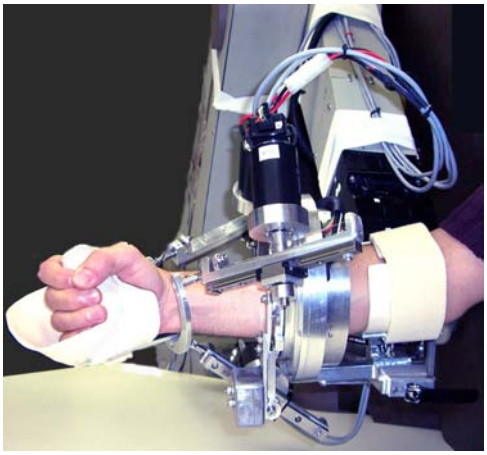

Figure 9. Subject operating the integrated MIME- *RiceWrist* System.

Mechanical Performance of the *RiceWrist*

Table 1 shows the workspace for the *RiceWrist* in terms of the range of motion about each of the three primary axis and torque display capability. The singularity-free workspace of the *RiceWrist* is 100% of the average human joint range of motion except for palmar flexion and dorsiflexion where it is 60%. The torque capabilities lag behind human abilities due to the limitations in current actuator technology, MIME robot loading restrictions and other practical restrictions on the size of arm exoskeleton actuators. Abduction/adduction is represented by α, and flexion/extension by β.

Figure 10 shows the manipulability of the *RiceWrist* measured as the absolute determinant of the inverse Jacobian [23]. Manipulability of a robot is a quantitative measure that captures the ease with which the device can arbitrarily change po-

Table 1. Comparison of workspace and torque limits of human arm and joints.

Joint	**Human Isometric Strength**[1]	**Human Joint Workspace Limits**	**Peak Torque Output Capability**	**Workspace Capability**
Forearm Supination/Pronation	9.1 Nm	Supination: 86° Pronation: 71°	5.08 Nm	Supination: 90° Pronation: 90°
Wrist Palmar/Dorsal Flexion	19.8 Nm	Palmar Flexion: 73° Dorsiflexion: 71°	$\approx$ 5.3 Nm	Palmar Flexion: 42° Dorsiflexion: 42°
Wrist Abduction/Adduction	20.8 Nm	Adduction: 33° Abduction: 19°	$\approx$ 5.3 Nm	Adduction: $>$ 33° Abduction: $>$ 19°

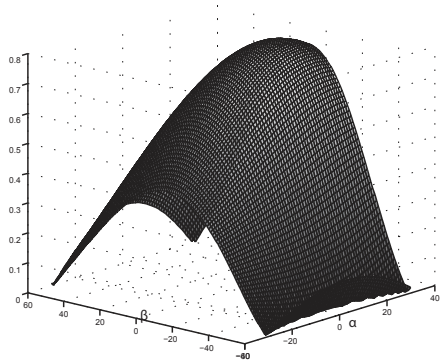

Figure 10. Manipulability of the wrist mechanism: α – abduction/adduction; β – flexion/extension.

sition and orientation from a given posture. For the *RiceWrist*, the manipulability measure is greatest in the center of the workspace, with the wrist at 0° of abduction/adduction (α) and flexion/extension (β). Manipulability, as expected, is low at the extents of each joint range of motion, although more so for flexion/extension.

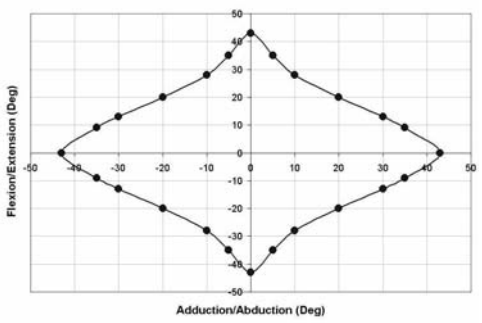

Figure 11. Range of motion for the *RiceWrist*

As shown in Figure 11, compound movements of the wrist remain singularity-free albeit with some reduction in the range of motion similar to the human wrist case. The compound movements of the wrist do not interfere with the forearm range of motion. Thus the *RiceWrist* provides adequate torque and range of motion for distal upper extremity rehabilitation for stroke therapy.

Controller Performance of the *RiceWrist*

Figure 12 presents the experimental results when the *RiceWrist* is operating in the Passive Mode. Subfigures 12(a)–(d) depict the trajectories for the four different joints, namely the wrist axes I, II, III, and forearm. Passive mode employs decoupled joint level trajectory controllers for each actuated axis. The solid lines in the figures represent the desired (commanded) trajectories, which are computed through linear interpolation between the specified initial and final joint positions. The dashed lines represent the experimentally recorded trajectories when the *RiceWrist* is operating freely. Finally, the dotted lines represent the experimentally recorded trajectories when the *RiceWrist* is worn by a human subject. The close match among the desired and experimentally observed trajectories imply adequate disturbance rejection characteristics of the implemented controllers.

CONCLUSIONS

This paper presents the *RiceWrist*, a four degree-of-freedom upper extremity rehabilitation robot for stroke therapy. The design is modified from the MAHI exoskeleton and used in conjunction with the Mirror Image Movement Enabler (MIME) system to provide passive, triggered, and active-constrained operation modes for combined robotic therapy protocols for comprehensive shoulder through wrist rehabilitation. The human isometric design specifications for range of motion and torque are experimentally verified. The three unilateral modes of operation of the MIME system and a therapist graphical user interface are implemented and demonstrated on the *RiceWrist*. Now that the mechanical system and the coding for the three therapy modes

[1]Source: Tsagarakis et al. [24]

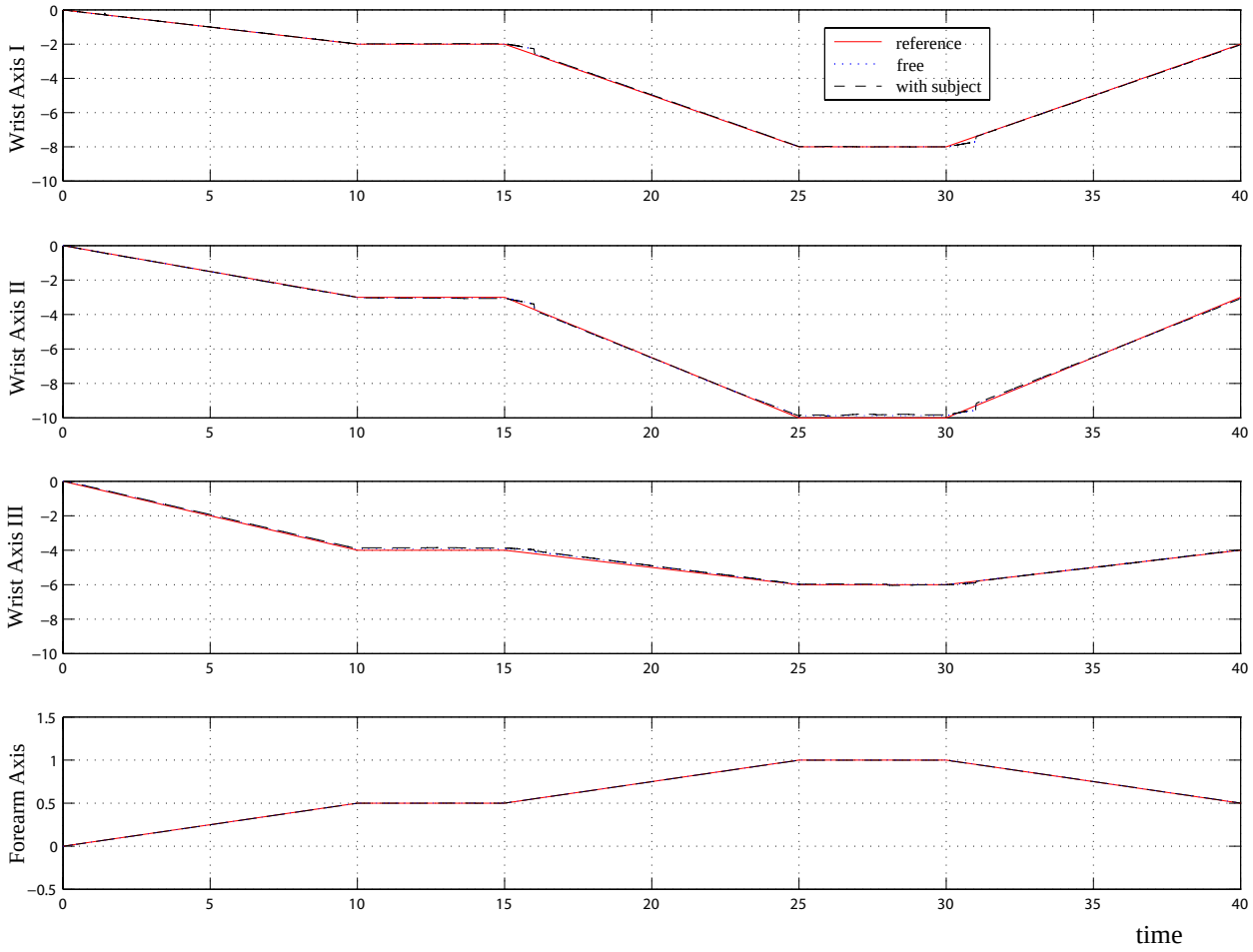

Figure 12. Experimental results for the *RiceWrist* operating in the Passive mode

are complete, the *RiceWrist* will go through preliminary user testing with healthy subjects followed by clinical trials.

ACKNOWLEDGMENT

This work is supported in part by a grant from the Central Texas Veterans Health Care System (CTVHCS) VA V674P-3804.

REFERENCES

[1] Gresham, G. H., 1990. "Past Achievements and New Directions in Stroke Outcome Research". *Stroke*, **21 (9 Suppl):II**, pp. 1–2.

[2] Wolf, P. A., D'Agostino, R. B., O'Neal, M. A., Sytkowski, P., Kase, C. S., Belanger, A. J., and Kannel, W. B., 1992. "Secular Trends in Stroke Incidence and Mortality: The Framingham Study". *Stroke*, **23**, pp. 1551–1555.

[3] Gresham, G. E., Alexander, D., Bishop, D. S., Giuliani, C., Goldberg, G., Holland, A., Kelly-Hayes, M., Linn, R. T., Roth, E. J., Stason, W. B., and Trombly, C. A., 1997. "Rehabilitation". *Stroke*, **28**(7), pp. 1522–1526.

[4] Erlandson, R. F., 1992. "Applications of Robotic/Mechatronic Systems in Special Education, Rehabilitation Therapy". *IEEE Trans. Rehab. Eng.*, **3**(1), pp. 22–34.

[5] Reinkensmeyer, D. J., Dewald, J. P. A., and Rymer, W. Z., 1996. "Robotic Devices for Physical Rehabilitation of Stroke Patients: Fundamental Requirements, Target Therapeutic Techniques, and Preliminary Designs.". *Technology and Disability*, **5**, pp. 205–215.

[6] Reinkensmeyer, D. J., Takahashi, C. D., Timoszyk, W. K., Reinkensmeyer, A. N., and Kahn, L. E., 2000. "Design of Robot Assistance for Arm Movement Therapy Following Stroke". *Advanced Robotics*, **14**(7), pp. 625–637.

[7] Khalili, D., and Zomlefer, M., 1988. "An Intelligent Robotic System for Rehabilitation of Joints and Estimation of Body Segment Parameters". *IEEE Trans. Biomed. Eng.*,

35(2), pp. 138–146.

[8] Goodall, R. M., Pratt, D. J., Rogers, C. T., and Murray-Leslie, C. M., 1987. "Enhancing Postural Stability in Hemi-Plegics Using Externally Applied Forces". *Intl. J. of Rehab. Research (suppl 5)*, **10**(4), pp. 132–140.

[9] White, C. J., Scneider, A. M., and Brogan Jr., W. K., 1993. "Robotic Orthosis for Stroke Patient Rehabilitation". In IEEE Intl. Conf. Eng. Med. Biol., pp. 1272–1273.

[10] Dirette, D., and Hinojosa, J., 1994. "Effects of Continuous Passive Motion on the Edematous Hands of Two Persons with Flaccid Hemiplegia". *American Journal of Occupational Therapy*, **48**(5), pp. 403–409.

[11] Burgar, C. G., Lum, P., Shor, P. C., and Van der Loos, H. F. M., 2000. "Development of Robots for Rehabilitation Therapy: The Palo Alto VA/Stanford Experience". *Journal of Rehabilitation Research and Development*, **37**(6), pp. 663–673.

[12] Fasoli, S. E., Krebs, H. I., and Hogan, N., 2004. "Robotic Technology and Stroke Rehabilitation". *Topics in Stroke Rehabilitation*, **11**, pp. 11–19.

[13] Hogan, N., and Krebs, H. I., 2004. "Interactive Robots for Neurorehabilitation". *Restorative Neurology and Neuroscience*, **22**, pp. 349–358.

[14] Reinkensmeyer, D. J., Emken, J. L., and Cramer, S. C., 2004. "Robotics, Motor Learning and Neurologic Recovery". *Annual Reviews in Biomedical Engineering*, **6**, pp. 497–525.

[15] Riener, R., Nef, T., and Colombo, G., 2005. "Robot-Aided Neurorehabilitation of the Upper Extremeties". *Medical and Biological Engineering and Computing*, **43**, pp. 2–10.

[16] Stein, J., 2004. "Motor Recovery Strategies after Stroke". *Topics in Stroke Rehabiliation*, **11**, pp. 12–22.

[17] O'Malley, M. K., Ro, T., and Levin, H. S., 2006. "Assessing and Inducing Neuroplasticity with TMS and Robotics". *Archives of PMR, Special Issue on Neuroplasticity and Neuroimaging in Acquired Brain Injury: Measurements, Concepts, and Applications*. in review.

[18] Charles, S. K., Krebs, H. I., Volpe, B. T., Lynch, D., and Hogan, N., 2005. "Wrist Rehabilitation Following Stroke: Initial Clinical Results". In International Conference on Rehabilitation Robotics, pp. 13–16.

[19] Hesse, S., Schulte-Tigges, G., Konrad, M., Bardeleben, A., and Werner, C., 2003. "Robot Assisted Arm Trainer for the Passive and Active Practice of Bilateral Forearm and Wrist Movements in Hemiparetic Subjects". *Archives of Physical Medicine and Rehabilitation*, **84**(6), pp. 915–920.

[20] Gupta, A., and O'Malley, M. K., 2006. "Design of a Haptic Arm Exoskeleton for Training and Rehabilitation". *IEEE/ASME Trans. Mechatron.*, **11**(3).

[21] Sledd, A., and O'Malley, M. K., 2006. "Performance Enhancement of a Haptic Arm Exoskeleton". In Int'l Sympo. Haptic Interfaces for Virtual Environ. Teleop. Syst., pp. 375–381.

[22] Lee, K. M., and Shah, D. K., 1988. "Kinematic Analysis of a Three Degrees-of-Freedom in-Parallel Actuated Manipulator". *IEEE Trans. Robot. Automat.*, **4**(3), June, pp. 354–360.

[23] Yoshikawa, T., 1985. "Manipulability of Robotic Mechanisms". *Int'l J. Robot. Research*, **4**(2), pp. 3–9.

[24] Tsagarakis, N., Caldwell, D. G., and Medrano-Cerda, G., 1999. "A 7DOF Pneumatic Muscle Actuator Powered Exoskeleton". In Int'l Workshop Robot and Human Interact. Commun., pp. 327–333.